Allen-Cahn and Cahn-Hilliard Variational Inequalities Solved with Optimization Techniques

Luise Blank, Martin Butz, Harald Garcke,
Lavinia Sarbu and Vanessa Styles

Abstract. Parabolic variational inequalities of Allen-Cahn and Cahn-Hilliard type are solved using methods involving constrained optimization. Time discrete variants are formulated with the help of Lagrange multipliers for local and non-local equality and inequality constraints. Fully discrete problems resulting from finite element discretizations in space are solved with the help of a primal-dual active set approach. We show several numerical computations also involving systems of parabolic variational inequalities.

Mathematics Subject Classification (2000). 35K55, 35S85, 65K10, 90C33, 90C53, 49N90, 65M60.

Keywords. Optimization, Phase-field method, Allen-Cahn model, Cahn-Hilliard model, variational inequalities, active set methods.

1. Introduction

Interface evolution can be described with the help of phase field approaches, see, e.g., [12]. An interface, in which a phase field or order parameter rapidly changes its value, is modelled to have a thickness of order ε, where $\varepsilon > 0$ is a small parameter. The model is based on the non-convex Ginzburg-Landau energy E which has the form

$$E(u) := \int_\Omega \left(\tfrac{\gamma\varepsilon}{2}|\nabla u|^2 + \tfrac{\gamma}{\varepsilon}\psi(u) \right) dx \,, \tag{1.1}$$

where $\Omega \subset \mathbb{R}^d$ is a bounded domain, $\gamma > 0$ is a parameter related to the interfacial energy and $u : \Omega \to \mathbb{R}$ is the phase field variable, also called order parameter. The

different phases correspond to the values $u = \pm 1$. In interfacial regions solutions rapidly change from values close to 1 to values close to -1 and the thickness of this interfacial region is proportional to the parameter ε. The potential function ψ can be a smooth double well potential, e.g., $\psi(u) = (1 - u^2)^2$ or an obstacle potential, e.g.,

$$\psi(u) = \psi_0(u) + I_{[-1,1]}(u) \,, \tag{1.2}$$

where $\psi_0 = \frac{1}{2}(1 - u^2)$ or another smooth, non-convex function and $I_{[-1,1]}$ is the indicator function, for the interval $[-1,1]$. The interface evolution is then given by the gradient flow equation, i.e., the phase field tries to minimize the energy in time with respect to an inner product corresponding to a vector space $\mathbf{Z}$. More specifically we obtain

$$\partial_t u(t) = -\mathrm{grad}_{\mathbf{Z}} E(u(t)) \,. \tag{1.3}$$

Considering a scaled L^2-inner product and the obstacle potential we obtain the *Allen-Cahn variational inequality*

$$(\varepsilon \partial_t u, \chi - u) + \gamma \varepsilon (\nabla u, \nabla(\chi - u)) + \tfrac{\gamma}{\varepsilon}(\psi_0'(u), \chi - u) \geq 0 \,, \tag{1.4}$$

which has to hold for almost all t and all $\chi \in H^1(\Omega)$ with $|\chi| \leq 1$. Here and in the following $(.,.)$ denotes the L^2-inner product. The mass-conserving H^{-1}-inner product yields in the obstacle case the fourth-order *Cahn-Hilliard variational inequality*:

$$\partial_t u = \Delta w \quad \text{a.e.}, \tag{1.5}$$

$$(w - \tfrac{\gamma}{\varepsilon}\psi_0'(u), \xi - u) \leq \gamma \varepsilon (\nabla u, \nabla(\xi - u)) \quad \forall \, \xi \in H^1(\Omega), |\xi| \leq 1, \tag{1.6}$$

together with $|u| \leq 1$ a.e. For these formulations it can be shown that under Neumann boundary conditions for w and initial conditions for u a unique solution (u, w) of (1.5)-(1.6) exists where u is H^2-regular in space, see [8, 4].

Using the H^2-regularity the formulation (1.4) and (1.5), (1.6) can be restated in the *complementary form*, where the equalities and inequalities have to hold almost everywhere:

$$\varepsilon \partial_t u = \gamma \varepsilon \Delta u - \tfrac{1}{\varepsilon}(\gamma \psi_0'(u) + \mu) \,, \tag{1.7}$$

respectively

$$\partial_t u = \Delta w \,, \quad w = -\gamma \varepsilon \Delta u + \tfrac{1}{\varepsilon}(\gamma \psi_0'(u) + \mu) \,, \tag{1.8}$$

$$\mu = \mu_+ - \mu_-, \ \mu_+ \geq 0, \ \mu_- \geq 0, \quad |u| \leq 1, \tag{1.9}$$

$$\mu_+(u - 1) = 0, \ \mu_-(u + 1) = 0 \,, \tag{1.10}$$

and homogeneous Neumann boundary conditions for u and w together with an initial phase distribution $u(0) = u_0$. Here, $\frac{1}{\varepsilon}\mu$ can be interpreted as a scaled Lagrange multiplier for the pointwise box-constraints. The scaling of the Lagrange multiplier μ with respect to ε is motivated by formal asymptotic expansions for obstacle potentials, see Blowey and Elliott [10] and Barrett, Garcke and Nürnberg [2]. Our scaling guarantees that μ is of order one. If we replace $\frac{1}{\varepsilon}\mu$ by μ in (1.7) we would observe a severe ε-dependence of μ. In practice this often results in oscillations in the primal-dual active set method for the discretized problem. In

fact iterates would oscillate between the bounds ± 1 and no convergence takes place.

For an arbitrary constant $c > 0$ we introduce the *primal-dual active sets* employing the primal variable u and the dual variable μ

$$A_+(t) = \{x \in \Omega \mid c(u-1) + \mu > 0\}, \qquad A_-(t) = \{x \in \Omega \mid c(u+1) + \mu < 0\}$$

and the inactive set $I := \Omega \setminus (A_+ \cup A_-)$. The restrictions (1.9)–(1.10) can now be reformulated as

$$u(x) = \pm 1 \text{ for almost all } x \in A_\pm, \quad \mu(x) = 0 \text{ for almost all } x \in I. \qquad (1.11)$$

A discrete version of (1.11) will lead later on to the primal-dual active set algorithm (PDAS).

Another reformulation of (1.9)–(1.10) is given with the help of a *non-smooth equation* as follows

$$H(u, \mu) := \mu - (\max(0, \mu + c(u-1)) + \min(0, \mu + c(u+1))) = 0, \qquad (1.12)$$

which allows us to interpret the following PDAS-method for the discretized problem as a semi-smooth Newton method and provides then local convergence, see [17], for a different context.

Given discrete times $t_n = n\tau, n \in \mathbb{N}_0$, where $\tau > 0$ is a given time step, and denoting by u^n an approximation of $u(t_n, \cdot)$, the backward Euler discretization of the gradient flow equation (1.3) is given as

$$\tfrac{1}{\tau}(u^n - u^{n-1}) = -\text{grad}_{\mathbf{Z}} E(u(t)). \qquad (1.13)$$

This time discretization has a natural variational structure. In fact one can compute a solution u^n as the solution of the minimization problem

$$\min_{|u| \leq 1} \left\{ E(u) + \tfrac{1}{2\tau} \|u - u^{n-1}\|_{\mathbf{Z}}^2 \right\}. \qquad (1.14)$$

One hence tries to decrease the energy E whilst taking into account the fact that deviations from the solution at the old time step costs, where the cost depends on the norm on $\mathbf{Z}$.

In particular for the Cahn-Hilliard formulation we obtain a non-standard PDE-constraint optimization problem as follows

$$\min \left\{ \tfrac{\gamma\varepsilon}{2} \int_\Omega |\nabla u|^2 + \tfrac{\gamma}{\varepsilon} \int_\Omega \psi_0(u) + \tfrac{\tau}{2} \int_\Omega |\nabla v|^2 \right\} \qquad (1.15)$$

such that

$$\Delta v = \tfrac{1}{\tau}(u - u^{n-1}) \text{ a.e.}, $$
$$|u| \leq 1 \text{ a.e.}, \quad \int_\Omega u = m, \qquad (1.16)$$

with

$$\tfrac{\partial v}{\partial n} = 0 \text{ a.e. on } \partial\Omega \text{ and } \int_\Omega v = 0.$$

This formulation has the form of an optimal control problem where u is the control and v is the state. In particular one has the difficulty that L^2-norms of gradients

enter the cost functional. We also remark that the non-local mean value constraints appear since the Cahn-Hilliard evolution variational inequality conserves mass. It turns out that the Lagrange multiplier w for the PDE equality constraint (1.16) equals v up to a constant, see also [16]. We hence obtain the reduced KKT-system (1.17)–(1.19), see [4] for details:

$$\frac{1}{\tau}(u - u^{n-1}) \;=\; \Delta w \text{ in } \Omega, \; \frac{\partial w}{\partial n} = 0 \text{ on } \partial\Omega, \qquad (1.17)$$

$$w + \gamma\varepsilon\Delta u - \frac{\gamma}{\varepsilon}\psi_0'(u) - \frac{1}{\varepsilon}\mu \;=\; 0 \quad \text{in } \Omega, \; \frac{\partial u}{\partial n} = 0 \text{ on } \partial\Omega, \qquad (1.18)$$

$$u(x) = \pm 1 \quad \text{if } x \in A_\pm, \qquad\qquad \mu(x) = 0 \quad \text{if } x \in I, \qquad (1.19)$$

where all equalities and inequalities have to hold almost everywhere. This system is a time discretization of the Cahn-Hilliard model (1.8), (1.11). We obtain a corresponding system for the time discretized Allen-Cahn variational inequality.

2. Primal-dual active set method (PDAS method)

The idea is now to apply the PDAS-algorithm (see below) to (1.14). However as is known for control problems with state constraint and for obstacle problems this strategy is not applicable in functions space as the iterates for the Lagrange multiplier μ are in general only measures. Therefore we apply the method to the fully discretized problems. Since we consider here evolution processes, where good preinitialization is available from the previous time steps, we avoid additional regularization or penalization techniques (see [19, 22, 23]) and still numerically obtain mesh independence.

We now use a finite element approximation in space with piecewise linear, continuous finite elements S_h with nodes $p_1, \ldots, p_{J_h}$ and nodal basis function $\chi_j \in S_h, j \in \mathcal{J}_h := \{1, \ldots, J_h\}$, and introduce a mass lumped inner product $(.,.)_h$. We can then formulate a discrete primal-dual active set method for iterates $(u^{(k)}, \mu^{(k)}) \in S_h \times S_h$ based on active nodes with indices $\mathcal{A}_\pm^{(k)}$ and inactive nodes with indices $\mathcal{I}^{(k)}$ as follows.

Primal-Dual Active Set Algorithm (PDAS):

1. Set $k = 0$, initialize $\mathcal{A}_\pm^{(0)}$ and define $\mathcal{I}^{(0)} = \mathcal{J}_h \setminus (\mathcal{A}_+^{(0)} \cup \mathcal{A}_-^{(0)})$.
2. Set $u^{(k)}(p_j) = \pm 1$ for $j \in \mathcal{A}_\pm^{(k)}$ and $\mu^{(k)}(p_j) = 0$ for $j \in \mathcal{I}^{(k)}$.
3. Solve the fully discretized version of the coupled system of PDEs (1.17)–(1.18), respectively of the system (1.7) to obtain $u^{(k)}(p_j)$ for $j \in \mathcal{I}^{(k)}$, $\mu^{(k)}(p_j)$ for $j \in \mathcal{A}_+^{(k)} \cup \mathcal{A}_-^{(k)}$ and $w^{(k)} \in S_h$.
4. Set $\mathcal{A}_+^{(k+1)} := \{j \in \mathcal{J}_h \mid c(u^{(k)}(p_j) - 1) + \mu^{(k)}(p_j) > 0\}$,
   $\mathcal{A}_-^{(k+1)} := \{j \in \mathcal{J}_h \mid c(u^{(k)}(p_j) + 1) + \mu^{(k)}(p_j) < 0\}$ and
   $\mathcal{I}^{(k+1)} := \mathcal{J}_h \setminus (\mathcal{A}_+^{(k+1)} \cup \mathcal{A}_-^{(k+1)})$.
5. If $\mathcal{A}_\pm^{(k+1)} = \mathcal{A}_\pm^{(k)}$ stop, otherwise set $k = k + 1$ and goto 2.

In the above algorithm Step 3 can be split into two steps. The first is to solve for u and w and the second is to determine μ. We give the details only for the

Cahn-Hilliard problem. For the Allen-Cahn formulation there is a corresponding system.

3a. Solve for $w^{(k)} \in S_h$ and $u^{(k)}(p_j)$ with $j \in \mathcal{I}^{(k)}$, the system

$$\frac{1}{\tau}(u^{(k)} - u_h^{n-1}, \chi)_h + (\nabla w^{(k)}, \nabla \chi) = 0 \qquad \forall \, \chi \in S_h, \qquad (2.1)$$

$$(w^{(k)}, \tilde{\chi})_h - \gamma \varepsilon (\nabla u^{(k)}, \nabla \tilde{\chi}) - \frac{\gamma}{\varepsilon}(\psi_0'(u_h^*), \tilde{\chi})_h = 0 \qquad \forall \, \tilde{\chi} \in \tilde{S}^{(k)} \qquad (2.2)$$

$$\text{with } \tilde{S}^{(k)} := \operatorname{span} \{\chi_i \mid i \in \mathcal{I}^{(k)}\}.$$

3b. Define $\mu^{(k)}$ on the active sets such that for all $j \in \mathcal{A}^{(k)}$

$$\mu^{(k)}(p_j)\,(1, \chi_j)_h = (\varepsilon w^{(k)} - \gamma \psi_0'(u_h^*), \chi_j)_h - \gamma \varepsilon^2 (\nabla u^{(k)}, \nabla \chi_j). \qquad (2.3)$$

In the above we either consider an implicit or an explicit discretization of the term $\psi_0'(u)$, i.e., we choose $\psi_0'(u_h^*)$ where $* \in \{n-1, n\}$. Figure 1 shows the structure of the system. The discretized elliptic equation (2.1) for $w^{(k)}$ is defined on the whole of $\mathcal{J}_h$ whereas the discrete elliptic equation (2.2) is defined only on the inactive set corresponding to $\mathcal{I}^{(k)}$ which is an approximation of the interface. The two equations are coupled in a way which leads to an overall symmetric system which will be used later when we propose numerical algorithms. For the Allen-Cahn system we have to solve (1.7) only on the approximated interface.
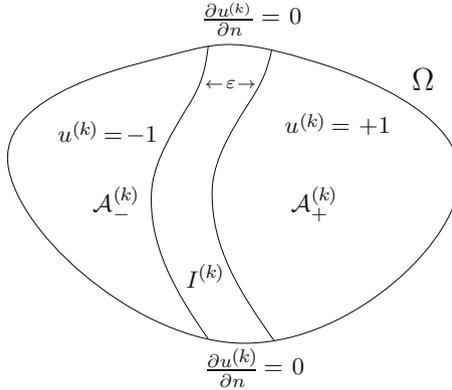

FIGURE 1. Structure of active and inactive sets.

3. Results for the Cahn-Hilliard variational inequality

It can be shown, see [4] for details, that the following results hold.

Lemma 3.1. *For all $u_h^{n-1} \in S_h$ and $\mathcal{A}_{\pm}^{(k)}$ there exists a unique solution $(u^{(k)}, w^{(k)}) \in S^h \times S^h$ of (2.1)-(2.2) with $* = (n-1)$ provided that $\mathcal{I}^{(k)} = \mathcal{J}_h \setminus (\mathcal{A}_+^{(k)} \cup \mathcal{A}_-^{(k)}) \neq \emptyset$.*
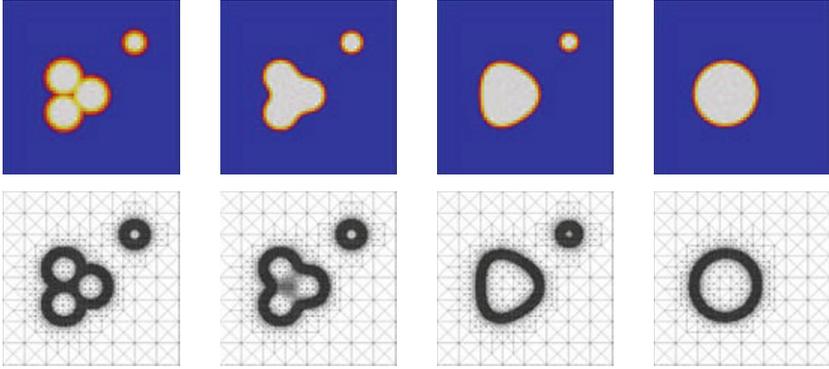
FIGURE 2. The upper row shows the evolution of the concentration and the lower row shows the corresponding meshes.

The assumption $\mathcal{I}^{(k)} \neq \emptyset$ guarantees that the condition $\fint_{\Omega} u^{(k)} = m$ can be fulfilled. Otherwise (2.1) may not be solvable. Furthermore we have shown in [4] using the equivalence of the PDAS-algorithm to a semi-smooth Newton method:

Theorem 3.2. *The primal-dual active set algorithm (PDAS) converges locally.*

Global convergence is not of large interest here, as we study a discrete time evolution and hence we always have good starting values from the previous time-step. However, the appropriate scaling of the Lagrange multiplier μ by $\frac{1}{\varepsilon}$, or respectively the choice of the parameter c is essential to avoid oscillatory behaviour due to bilateral constraints (see [4, 5]).

As far as we can compare the results with other methods the PDAS-method outperformed previous approaches, see [4]. One of the bottle necks for a speed-up is the linear algebra solver. The linear system to be solved is symmetric and has a saddle point structure. Efficient preconditioning of the system is difficult and has to be addressed in the future.

Finally let us mention further methods to solve Cahn-Hilliard variational inequalities. It is also possible to use a projected block Gauss-Seidel type scheme to solve the variational inequality directly and hence at each node a variational inequality for a vector with two components has to be solved. Another approach is a splitting method due to Lions and Mercier [21] (see [9], [4]) and Gräser and Kornhuber [16] use preconditioned Uzawa-type iterations coupled to a monotone multigrid method. The latter approach is similar to our approach as it is also an active set approach. Although, unlike our approach, Gräser and Kornhuber [16] have to solve a second-order variational inequality in each step in order to update the active set. Finally, we also mention a recent multigrid method of Banas and Nürnberg [1] and an approach based on regularization by Hintermüller, Hinze and Tber [18].

(a) $n = 0$ (b) $n = 50$ (c) $n = 100$ (d) $n = 300$
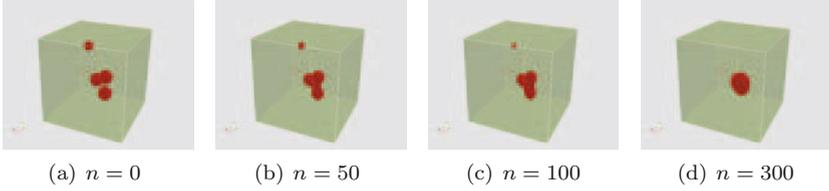
FIGURE 3. 3d simulation with 4 spheres as initial data on an adaptive mesh.
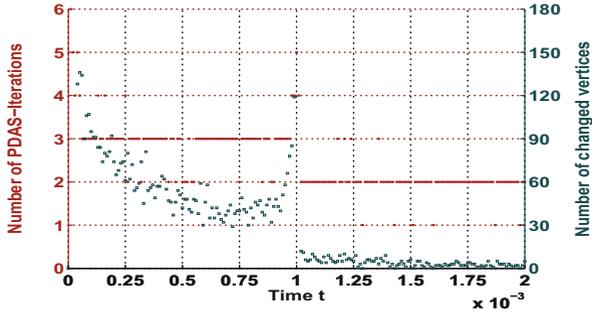

FIGURE 4. PDAS-iterations count per time step for the 2d simulation in Figure 2.

4. Results for the Allen-Cahn variational inequality

4.1. Scalar Allen-Cahn problem without local constraints

If we consider interface evolution given by the Allen-Cahn variational inequality (1.4) we obtain corresponding results to the Cahn-Hilliard problem. However, the L^2-inner product does not conserve the mass, and hence, e.g., given circles or spheres as initial data they will vanish in finite time. For the example of a shrinking circle we discuss the issue of mesh independence of the PDAS-method applied to the fully discretized problem. The number of PDAS iterations might depend on the mesh size h. There is still a lack of analytical results. However, we can investigate this numerically comparing various uniform meshes of a maximal diameter h. We choose the radius 0.45 of the circle at $t = 0$. The time where the circle disappears is 0.10125. Table 1 shows the average number of PDAS iterations up to $t = 0.03$ for fixed $\varepsilon = \frac{1}{16\pi}$. In the third column we list the results fixing also $\tau = 5 \cdot 10^{-4}$. Although the number of PDAS iterations increases for smaller mesh size, this increase is only by a factor of approximately 1.3. However, in our applications the time step τ and the space discretization are in general coupled. Hence it is more appropriate to look at the number of Newton iterations when both τ and h are driven to zero. We see in the last column that the iteration number is almost constant. This is due to the time evolution, since good initial data on the current time step are given from the solution of the previous time step. Hence our numerical

investigations indicate that the proposed method is mesh independent for this setting. We remark that Table 1 shows the average number of Newton iterations. There might be situations, in particular if one starts with irregular initial data, where a slight dependence of the number of Newton iterations on the time step size is possible for certain time steps. In all our simulations we hardly observed a mesh dependence of the number of Newton iterations even for irregular initial data if time step and space step size were reduced simultaneously. An analytical result showing mesh independence for arbitrary initializations is however not available.

h	DOFs	PDAS iter. ø for $\tau = 5 \cdot 10^{-4}$	τ	PDAS iter. ø for varying τ
1/128	66049	2.57	$1 \cdot 10^{-3}$	3.20
1/256	263169	3.10	$5 \cdot 10^{-4}$	3.10
1/512	1050625	4.02	$2.5 \cdot 10^{-4}$	3.30
1/1024	4198401	5.18	$1.25 \cdot 10^{-4}$	3.37

TABLE 1. Average number of PDAS iterations.

4.2. Scalar Allen-Cahn problem with mass constraint

While the Cahn-Hilliard approach incorporates mass conservation by using the H^{-1}-norm, we can also use the L^2-norm and enforce in addition the mass conservation as a non-local constraint during the gradient flow. This leads to the Allen-Cahn variational inequality (1.4) with the additional constraint $\fint_\Omega u dx := \frac{1}{|\Omega|}\int_\Omega u dx = m$ where $m \in (-1,1)$ is the mean value of the initial data u_0. We can introduce for this constraint a Lagrange multiplier λ and we can restate the problem as

$$\varepsilon \partial_t u = \gamma \varepsilon \Delta u - \frac{1}{\varepsilon}(\gamma \psi_0'(u) + \mu - \lambda) \text{ a.e.}, \tag{4.1}$$

$$\fint_\Omega u dx = m \qquad \text{for almost all } t \in [0,T], \tag{4.2}$$

where also the complementarity conditions (1.9)–(1.10) hold.

Using a penalty approach for the inequality constraints and projecting the mass constraint we have shown in [5] the existence, uniqueness and regularity of the solution of the KKT-system which is non-standard due to the coupling of non-local equality and local inequality constraints.

Theorem 4.1. *Let $T > 0$ and Ω be a domain which is bounded and either convex or has a $C^{1,1}$-boundary. Furthermore the initial data $u_0 \in H^1(\Omega)$ fulfill $|u_0| \leq 1$ a.e. and $\fint_\Omega u_0 = m$ for a given $m \in (-1,1)$. Then there exists a unique solution (u, μ, λ) of the KKT-system (4.1), (4.2), (1.9), (1.10) with $\mu \in L^2(\Omega_T)$, $\lambda \in L^2(0,T)$ and $u \in L^2(0,T;H^2(\Omega)) \cap L^\infty(0,T;H^1(\Omega)) \cap H^1(\Omega_T)$.*

Using the presented implicit time discretization (1.13) and the given finite element approximation with mass lumping we apply, similar as above, a PDAS algorithm. We define $m_j := (1, \chi_j)$ and $a_{ij} = (\nabla \chi_j, \nabla \chi_i)$ and denote by $u_j^{(k)}$ the coefficients of $u^{(k)} = \sum_{j \in \mathcal{J}_h} u_j^{(k)} \chi_j$. Then we obtain as Step 3:

3a. Solve for $u_j^{(k)}$ for $j \in \mathcal{I}^{(k)}$ and $\lambda^{(k)}$:

$$(\tfrac{\varepsilon}{\tau} - \tfrac{\gamma}{\varepsilon})m_j u_j^{(k)} + \gamma\varepsilon \sum_{i\in\mathcal{I}^{(k)}} a_{ij} u_i^{(k)} - \tfrac{1}{\varepsilon}m_j\lambda^{(k)} \qquad (4.3)$$

$$= \tfrac{\varepsilon}{\tau}m_j u_j^{n-1} + \gamma\varepsilon\Big(\sum_{i\in\mathcal{A}_-^{(k)}} a_{ij} - \sum_{i\in\mathcal{A}_+^{(k)}} a_{ij} \Big) \quad \forall j \in \mathcal{I}^{(k)},$$

$$\sum_{i\in\mathcal{I}^{(k)}} m_i u_i^{(k)} = m \sum_{i\in\mathcal{J}_h} m_i - \sum_{i\in\mathcal{A}_+^{(k)}} m_i + \sum_{i\in\mathcal{A}_-^{(k)}} m_i. \qquad (4.4)$$

3b. Define $\mu_j^{(k)}$ for $j \in \mathcal{A}_\pm^{(k)}$ using:

$$\mu_j^{(k)} = -(\tfrac{\varepsilon^2}{\tau} - \gamma)u_j^{(k)} - \gamma\varepsilon^2\tfrac{1}{m_j} \sum_{i\in\mathcal{J}_h} a_{ij} u_i^{(k)} + \lambda^{(k)} + \tfrac{\varepsilon^2}{\tau}u_j^{n-1}. \qquad (4.5)$$

Hence the main effort when applying the PDAS algorithm is solving the system (4.3)–(4.4) where the size $|\mathcal{I}^{(k)}|+1$ is given by the size of the approximated interface.

Like in the Cahn-Hilliard case we can show local convergence of the method by interpreting the algorithm as a Newton method. However using the presented implicit time discretization we obtain analytically the following restriction on the time step (see [5] Theorem 4.2):

$$\tau\Big(1 - \tfrac{\varepsilon^2}{c_h^p}\Big) < \tfrac{\varepsilon^2}{\gamma} \qquad (4.6)$$

where $c_h^p > 0$ is the Poincaré constant such that $(v,v)_h \le c_h^p(\nabla v, \nabla v)$ for all $v \in S^h$ with $\int_\Omega v = 0$ and $v(p_j) = 0$ for active nodes p_j. In [5] the size of c_h^p is discussed in more detail. For example in one dimension given a good numerical approximation of $\mathcal{I}$ no restriction at all has to be enforced for the time step τ. We can also use a semi-implicit discretization with a primal-dual active set algorithm. In this case no time restrictions have to be enforced for the algorithm. However it turns out that the fully implicit time discretization is much more accurate [5].

We give two numerical simulations. In Figure 5 we show interface evolution in two dimensions where the initial phase distribution is random and no pure phases are present. Already at time $t = 0.002$ grains start to form and grow and at $t = 0.003$ we have two phases separated by a diffuse interface. Now the interface moves according to motion by mean curvature but preserving the volume of both phases. That means that closed curves turn into circles and shapes with less volume shrink and disappear while at the same time shapes with the highest volume will grow. At the end (i.e., when the problem becomes stationary) there are three different shapes we can obtain: a circle, a quarter of a circle in one of the corners (see Figure 5) or a straight vertical or horizontal line dividing the two phases. The computation in Figure 6 presents the evolution for a dumbbell. Without the volume conservation the dumbbell would dissect and the two spheres
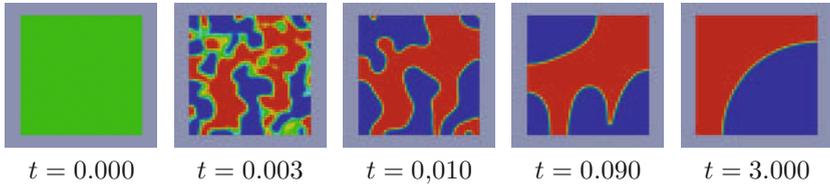
$t = 0.000$ $\qquad$ $t = 0.003$ $\qquad$ $t = 0,010$ $\qquad$ $t = 0.090$ $\qquad$ $t = 3.000$

FIGURE 5. Volume controlled Allen-Cahn equation (2d) with random initial data (varying between -0.1 and 0.1).

$t = 0.001$ $\qquad$ $t = 0.010$ $\qquad$ $t = 0.100$ $\qquad$ $t = 0.500$
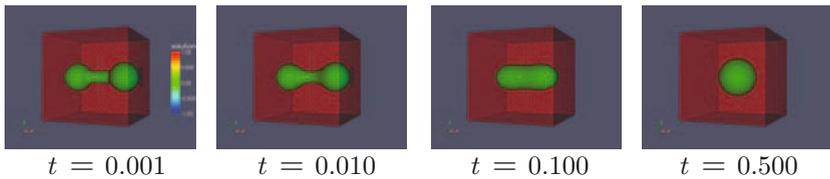
FIGURE 6. Volume controlled Allen-Cahn equation with a dumbbell as initial data.

would shrink and disappear. The volume conservation forces the dumbbell to turn into an ellipsoid before turning into a sphere and finally becoming stationary.

Finally, we briefly would like to mention that our approach can be used to solve problems in structural topology optimization. There the mean compliance penalized with the Ginzburg-Landau energy E (1.1) has to be minimized. The gradient approach can be seen as a pseudo time stepping approach and results in a time discretized Allen-Cahn variational inequality coupled with elasticity and mass constraints, which can be solved with the above method (see [5, 6, 3]).

4.3. Systems of Allen-Cahn variational inequalities

In many applications more than two phases or materials appear, see [11, 13] and the references therein. For numerical approaches to systems of Allen-Cahn variational inequalities we refer to [14, 15, 13] where explicit in time discretizations have been used, and to the work of Kornhuber and Krause [20] who discuss Gauss-Seidel and multigrid methods. In what follows we want to introduce a primal-dual active set method for systems of Allen-Cahn variational inequalities which in contrast to earlier approaches does not need an explicit handling of the geometry of the Gibbs simplex.

Therefore we introduce a concentration vector $\mathbf{u} = (u_1, \ldots, u_N)^T : \Omega \to \mathbb{R}^N$ with the property $u_i \geq 0$, $\sum_{i=1}^N u_i = 1$, i.e., $\mathbf{u}(x, t)$ lies on the Gibbs simplex

$$G := \{\boldsymbol{\xi} \in \mathbb{R}^N : \boldsymbol{\xi} \geq \mathbf{0}, \boldsymbol{\xi} \cdot \mathbf{1} = 1\}.$$

For the bulk potential $\psi : \mathbb{R}^N \to \mathbb{R}_0^+ \cup \{\infty\}$ we consider the multi-obstacle potential

$$\psi(\boldsymbol{\xi}) = \begin{cases} \psi_0(\boldsymbol{\xi}) := -\frac{1}{2}\boldsymbol{\xi} \cdot \mathbf{A}\boldsymbol{\xi} & \text{for } \boldsymbol{\xi} \geq \mathbf{0}, \boldsymbol{\xi} \cdot \mathbf{1} = 1, \\ \infty & \text{otherwise,} \end{cases} \tag{4.7}$$

with $\mathbf{A}$ being a symmetric constant $N \times N$ matrix. We remark that different phases which correspond to minima of ψ only occur if $\mathbf{A}$ has at least one positive eigenvalue. The total underlying non-convex energy is given similar to (1.1) by

$$E(\mathbf{u}) := \int_\Omega \left(\frac{\gamma\varepsilon}{2}|\nabla\mathbf{u}|^2 + \frac{\gamma}{\varepsilon}\psi(\mathbf{u}) \right) dx \,.$$

We also consider systems in which the total spatial amount of the phases are conserved. In this case one studies the steepest descent of E under the constraint $\fint_\Omega \mathbf{u}\, dx = \mathbf{m} = (m^1, \ldots, m^N)^T$ where $m^i \in (0,1)$ for $i \in \{1, \ldots, N\}$ is a fixed number. We now define

$$\mathcal{G}^\mathbf{m} := \{\mathbf{v} \in H^1(\Omega, \mathbb{R}^N) : \fint_\Omega \mathbf{v} = \mathbf{m}, \sum_{i=1}^N v_i = 1, \mathbf{v} \geq \mathbf{0}\}$$

and note that for $\mathbf{u} \in \mathcal{G}^\mathbf{m}$ it follows $\fint_\Omega \mathbf{u} - \mathbf{m} \in S := \{\mathbf{v} \in \mathbb{R}^N : \sum_{i=1}^N v_i = 0\}$. Then the interface evolution with mass conservation can be formulated as the following variational inequality: For given $\mathbf{u}_0 \in \mathcal{G}^\mathbf{m}$ find $\mathbf{u} \in L^2(0, T; \mathcal{G}^\mathbf{m}) \cap H^1(0, T; \mathbf{L}^2(\Omega))$ such that $\mathbf{u}(., 0) = \mathbf{u}_0$ and such that for almost all $t \in (0, T)$ it holds

$$\varepsilon(\tfrac{\partial\mathbf{u}}{\partial t}, \boldsymbol{\chi} - \mathbf{u}) + \gamma\varepsilon(\nabla\mathbf{u}, \nabla(\boldsymbol{\chi} - \mathbf{u})) - \tfrac{\gamma}{\varepsilon}(\mathbf{A}\mathbf{u}, \boldsymbol{\chi} - \mathbf{u}) \geq 0 \quad \forall \boldsymbol{\chi} \in \mathcal{G}^\mathbf{m}. \tag{4.8}$$

Our numerical approach again depends on a reformulation of (4.8) with the help of Lagrange multipliers. We introduce Lagrange multipliers $\boldsymbol{\mu}$ and Λ corresponding to the constraints $\mathbf{u} \geq \mathbf{0}$ and $\sum_{i=1}^N u_i = 1$ respectively. Taking into account the condition $\sum_{i=1}^N u_i = 1$ we use for the mass constraints the projected version $\mathbf{P}_S(\fint_\Omega \mathbf{u} - \mathbf{m}) = \mathbf{0}$, where $\mathbf{P}_S$ is a projection onto S and introduce for this condition a Lagrange multiplier $\boldsymbol{\lambda} \in S$. In [6] we prove the following theorem in which $\mathbf{L}^2(\Omega)$, $\mathbf{H}^1(\Omega)$, etc. denote spaces of vector-valued functions.

Theorem 4.2. *Let $\Omega \subset \mathbb{R}^d$ be a bounded domain and assume that either Ω is convex or $\partial\Omega \in C^{1,1}$. Let $\mathbf{u}_0 \in \mathcal{G}^\mathbf{m}$ such that $\int_\Omega \mathbf{u}_0 > \mathbf{0}$. Then there exists a unique solution* $(\mathbf{u}, \boldsymbol{\mu}, \boldsymbol{\lambda}, \Lambda)$ *with*

$$\mathbf{u} \in L^\infty(0, T; \mathbf{H}^1(\Omega)) \cap H^1(0, T; \mathbf{L}^2(\Omega)) \cap L^2(0, T; \mathbf{H}^2(\Omega)), \tag{4.9}$$

$$\boldsymbol{\mu} \in L^2(0, T; \mathbf{L}^2(\Omega)), \tag{4.10}$$

$$\boldsymbol{\lambda} \in \mathbf{L}^2(0, T) \text{ and } \sum_{i=1}^N \lambda_i = 0 \text{ for almost all } t \in (0, T), \tag{4.11}$$

$$\Lambda \in L^2(0, T; L^2(\Omega)) \tag{4.12}$$

such that on $\Omega_T := \Omega \times (0, T)$ we have

$$\varepsilon \frac{\partial \mathbf{u}}{\partial t} - \gamma \varepsilon \Delta \mathbf{u} - \frac{\gamma}{\varepsilon} \mathbf{A} \mathbf{u} - \frac{1}{\varepsilon} \boldsymbol{\mu} - \frac{1}{\varepsilon} \Lambda \mathbf{1} - \frac{1}{\varepsilon} \boldsymbol{\lambda} = \mathbf{0} \quad a.e. \ in \ \Omega_T, \tag{4.13}$$

$$\mathbf{u}(0) = \mathbf{u}_0, \ \frac{\partial \mathbf{u}}{\partial \nu} = \mathbf{0} \qquad a.e. \ on \ \partial\Omega \times (0, T), \tag{4.14}$$

$$\sum_{i=1}^{N} u_i = 1, \ \mathbf{u} \geq \mathbf{0}, \ \boldsymbol{\mu} \geq \mathbf{0} \quad a.e. \ in \ \Omega_T, \tag{4.15}$$

$$\mathbf{P}_S(\fint_{\Omega} \mathbf{u} - \mathbf{m}) = \mathbf{0}, \ (\boldsymbol{\mu}, \mathbf{u}) = 0 \quad for \ almost \ all \ t. \tag{4.16}$$

The proof is based on a penalty approach where the main difficulty is to show that approximations of the Lagrange multipliers $\boldsymbol{\mu}, \boldsymbol{\lambda}$ and Λ can be bounded. This issue is related to the question whether the constraints are in a suitable sense independent of each other. In order to show that Lagrange multipliers are unique one has to use some graph theory in order to show that the undirected graph with vertices $\{1, \ldots, N\}$ and edges $\{\{i, j\} \mid$ there is an interface between i and $j\}$ is connected.

Similar to the previous sections we now discretize (4.13)–(4.16) in time and space and we use a PDAS algorithm. However, for each component u_i we have to consider its own active and inactive sets $\mathcal{A}_i := \{j \in \mathcal{J}_h \mid c(u_i)_j + (\mu_i)_j < 0\}$ and $\mathcal{I}_i := \mathcal{J}_h \setminus \mathcal{A}_i$. In the following we use the notation

$$\mathbf{u}^{(k)} = \sum_{i=1}^{N} \sum_{j \in \mathcal{J}_h} (u_i^{(k)})_j \chi_j \mathbf{e}_i$$

for the kth iterate $\mathbf{u}^{(k)} \in (S_h)^N$ in the vector-valued PDAS algorithm.

Primal-Dual Active Set Algorithm (PDAS-Vector):

1. Set $k = 0$, initialize $\mathcal{A}_i^{(0)}$ and define $\mathcal{I}_i^{(0)} = \mathcal{J}_h \setminus \mathcal{A}_i^{(0)}$ for all $i \in \{1, \ldots, N\}$.
2. Set $(u_i^{(k)})_j = 0$ for $j \in \mathcal{A}_i^{(k)}$ and $(\mu_i^{(k)})_j = 0$ for $j \in \mathcal{I}_i^{(k)}$ for all $i \in \{1, \ldots, N\}$.
3a. To obtain $(\Lambda^{(k)})_j$ for all $j \in \mathcal{J}_h$, $\lambda_i^{(k)}$ for all $i \in \{1, \ldots, N-1\}$ and $(u_i^{(k)})_j$ for all $i = 1, \ldots, N$ and $j \in \mathcal{I}_i^{(k)}$ we solve

$$\frac{\varepsilon^2}{\tau}(u_i^{(k)})_j - \gamma \sum_{m=1}^{N} A_{im}(u_m^{(k)})_j + \frac{\gamma \varepsilon}{m_j} \sum_{l \in \mathcal{I}_i^{(k)}} a_{lj}(u_i^{(k)})_l - [\lambda_i^{(k)} + (\Lambda^{(k)})_j]$$

$$= \frac{\varepsilon^2}{\tau}(u_i^{n-1})_j, \quad i = 1, \ldots, N, j \in \mathcal{I}_i^{(k)}, \tag{4.17}$$

$$\sum_{j \in \mathcal{J}_h} m_j((u_i^{(k)})_j - (u_N^{(k)})_j) = \sum_{j \in \mathcal{J}_h} m_j(m^i - m^N), \ i = 1, \ldots, N-1,$$

$$\sum_{i=1}^{N}(u_i^{(k)})_j = 1, \quad j \in \mathcal{J}_h, \tag{4.18}$$

where we replace $\lambda_N^{(k)}$ by $\lambda_N^{(k)} = -\lambda_1^{(k)} - \cdots - \lambda_{N-1}^{(k)}$.

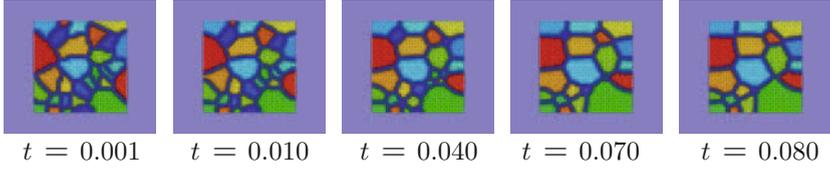| $t = 0.001$ | $t = 0.010$ | $t = 0.040$ | $t = 0.070$ | $t = 0.080$ |

FIGURE 7. Vector-valued Allen-Cahn variational inequality with a Voronoi partitioning as initial data (30 order parameters).

3b. Set $\lambda_N^{(k)} = -\lambda_1^{(k)} - \cdots - \lambda_{N-1}^{(k)}$ and determine the values

$$(\mu_i^{(k)})_j = \tfrac{\varepsilon^2}{\tau}(u_i^{(k)})_j - \gamma \sum_{m=1}^{N} A_{im}(u_m^{(k)})_j + \tfrac{\gamma\varepsilon^2}{m_j} \sum_{l \in \mathcal{J}_h} a_{lj}(u_i^{(k)})_l$$
$$- \lambda_i^{(k)} - \Lambda_j^{(k)} - \tfrac{\varepsilon^2}{\tau}(u_i^{n-1})_j$$

for $i = 1, \ldots, N$ and $j \in \mathcal{A}_i^{(k)}$.

4. Set $\mathcal{A}_i^{(k+1)} := \{j \in \mathcal{J}_h : c(u_i^{(k)})_j - (\mu_i^{(k)})_j < 0\}$ and
$\mathcal{I}_i^{(k+1)} := \mathcal{J}_h \setminus \mathcal{A}_i^{(k+1)}$.
5. If $\mathcal{A}_i^{(k+1)} := \mathcal{A}_i^{(k)}$ for all $i \in \{1, \ldots, N\}$ stop, otherwise set $k = k + 1$ and goto 2.

Remark 4.1. i) In each node p_j for $j \in \mathcal{J}_h$ some components are active and the others are inactive. The number of components which are active can vary from point to point. Only for each individual component can we split the set of nodes into nodes which are active (for this component) and its complement. The resulting linear system is hence quite complex but can be solved efficiently with the help of MINRES, see [7].

ii) There is a straightforward variant of (PDAS-Vector) without mass constraints. In this case we omit the first conditions in (4.18) and the Lagrange multipliers $\boldsymbol{\lambda} \in S$.

In Figure 7 we use a Voronoi partitioning algorithm to randomly define initial data in a 2d computational domain. We use 30 order parameters for this computation and show the time evolution in Figure 7. In Figure 8 we begin the computation with a sphere that is divided into three equal spherical wedges. Each of these wedges is represented by a different phase, i.e., we have three phases in the sphere and one phase outside. The evolution converges for large times to a triple bubble which is the least area way to separate three given volumes.
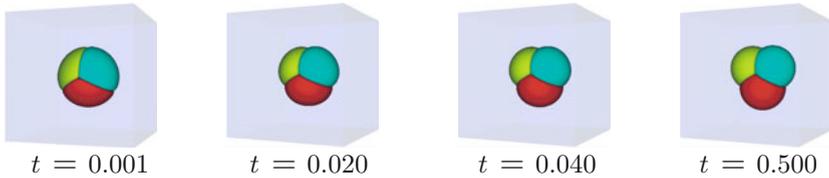
$t = 0.001$ $t = 0.020$ $t = 0.040$ $t = 0.500$

FIGURE 8. Triple bubble; vector-valued Allen-Cahn with volume constraints, 4 order parameter.

References

[1] L. Banas and R. Nürnberg, *A multigrid method for the Cahn-Hilliard equation with obstacle potential.* Appl. Math. Comput. **213** (2009), 290–303.

[2] J.W. Barrett, H. Garcke, and R. Nürnberg, *On sharp interface limits of Allen-Cahn/Cahn-Hilliard variational inequalities.* Discrete Contin. Dyn. Syst. S **1** (1) (2008), 1–14.

[3] L. Blank, H. Garcke, L. Sarbu, T. Srisupattarawanit, V. Styles, and A. Voigt, *Phase-field approaches to structural topology optimization*, a contribution in this book.

[4] L. Blank, M. Butz, and H. Garcke, *Solving the Cahn-Hilliard variational inequality with a semi-smooth Newton method*, ESAIM: Control, Optimization and Calculus of Variations, DOI: 10.1051/COCV/2010032.

[5] L. Blank, H. Garcke, L. Sarbu, and V. Styles, *Primal-dual active set methods for Allen-Cahn variational inequalities with non-local constraints.* DFG priority program 1253 "Optimization with PDEs", Preprint No. 1253-09-01.

[6] L. Blank, H. Garcke, L. Sarbu, and V. Styles, *Non-local Allen-Cahn systems: Analysis and a primal dual active set method.* Preprint No. 02/2011, Universität Regensburg.

[7] L. Blank, L. Sarbu, and M. Stoll, *Preconditioning for Allen-Cahn variational inequalities with non-local constraints.* Preprint Nr.11/2010, Universität Regensburg, Mathematik.

[8] J.F. Blowey and C.M. Elliott, *The Cahn-Hilliard gradient theory for phase separation with nonsmooth free energy I. Mathematical analysis.* European J. Appl. Math. **2**, no. 3 (1991), 233–280.

[9] J.F. Blowey and C.M. Elliott, *The Cahn-Hilliard gradient theory for phase separation with nonsmooth free energy II. Mathematical analysis.* European J. Appl. Math. **3**, no. 2 (1991), 147–179.

[10] J.F. Blowey and C.M. Elliott, *A phase-field model with a double obstacle potential.* Motion by mean curvature and related topis (Trento, 1992), 1–22, de Gruyter, Berlin 1994.

[11] L. Bronsard and F. Reitich, *On three-phase boundary motion and the singular limit of a vector-valued Ginzburg-Landau equation.* Arch. Rat. Mech. Anal. **124** (1993), 355–379.

[12] L.Q. Chen, *Phase-field models for microstructure evolution.* Annu. Rev. Mater. Res. 32 (2001), 113–140.

[13] H. Garcke, B. Nestler, B. Stinner, and F. Wendler, *Allen-Cahn systems with volume constraints.* Mathematical Models and Methods in Applied Sciences **18**, no. 8 (2008), 1347–1381.

[14] H. Garcke, B. Nestler, and B. Stoth. *Anisotropy in multi-phase systems: a phase field approach.* Interfaces Free Bound. **1** (1999), 175–198.

[15] H. Garcke and V. Styles. *Bi-directional diffusion induced grain boundary motion with triple junctions.* Interfaces Free Bound. **6**, no. 3 (2004), 271–294.

[16] C. Gräser and R. Kornhuber, *On preconditioned Uzawa-type iterations for a saddle point problem with inequality constraints.* Domain decomposition methods in science and engineering XVI, 91–102, Lect. Notes Comput. Sci. Engl. **55**, Springer, Berlin 2007.

[17] M. Hintermüller, K. Ito, and K. Kunisch, *The primal-dual active set strategy as a semismooth Newton method*, SIAM J. Optim. **13** (2002), no. 3 (2003), 865–888 (electronic).

[18] M. Hintermüller, M. Hinze, and M.H. Tber, *An adaptive finite element Moreau-Yosida-based solver for a non-smooth Cahn-Hilliard problem.* Matheon preprint Nr. 670, Berlin (2009), to appear in Optimization Methods and Software.

[19] K. Ito and K. Kunisch, *Semi-smooth Newton methods for variational inequalities of the first kind.* M2AN Math. Model. Numer. Anal. **37**, no. 1 (2003), 41–62.

[20] R. Kornhuber and R. Krause. *On multigrid methods for vector-valued Allen-Cahn equations with obstacle potential.* Domain decomposition methods in science and engineering, 307–314 (electronic), Natl. Auton. Univ. Mex., México, 2003.

[21] P.-L. Lions and B. Mercier, *Splitting algorithms for the sum of two non-linear operators.* SIAM J. Numer. Anal. **16** (1979), 964–979.

[22] C. Meyer, A. Rösch, and F. Tröltzsch, *Optimal control problems of PDEs with regularized pointwise state constraints.* Comput. Optim. Appl. **33**, (2006), 209–228.

[23] I. Neitzel and F. Tröltzsch, *On regularization methods for the numerical solution of parabolic control problems with pointwise state constraints.* ESAIM: COCV **15** (2) (2009), 426–453.

[24] A. Schmidt and K.G. Siebert, *Design of adaptive finite element software. The finite element toolbar.* ALBERTA, Lecture Notes in Computational Science and Engineering **42**, Springer-Verlag, Berlin 2005.

Luise Blank, Martin Butz and Harald Garcke
Fakultät für Mathematik, Universität Regensburg
D-93040 Regensburg, Germany
e-mail: luise.blank@mathematik.uni-r.de
        martin.butz@mathematik.uni-r.de
        harald.garcke@mathematik.uni-r.de

Lavinia Sarbu and Vanessa Styles
Department of Mathematics
University of Sussex
Brighton BN1 9RF, UK
e-mail: ls99@sussex.ac.uk
        v.styles@sussex.ac.uk